

Provided for non-commercial research and education use.
Not for reproduction, distribution or commercial use.



This article appeared in a journal published by Elsevier. The attached copy is furnished to the author for internal non-commercial research and education use, including for instruction at the authors institution and sharing with colleagues.

Other uses, including reproduction and distribution, or selling or licensing copies, or posting to personal, institutional or third party websites are prohibited.

In most cases authors are permitted to post their version of the article (e.g. in Word or Tex form) to their personal website or institutional repository. Authors requiring further information regarding Elsevier's archiving and manuscript policies are encouraged to visit:

<http://www.elsevier.com/copyright>



Contents lists available at ScienceDirect

Microelectronics Journal

journal homepage: www.elsevier.com/locate/mejo

A simple parallel conduction extraction method (SPCEM) for MODFETs and undoped GaN-based HEMTs

S.B. Lisesivdin^{a,b,*}, N. Balkan^a, E. Ozbay^{c,d}

^a Department of Computing and Electronic Systems, University of Essex, CO4 3SQ Colchester, UK

^b Department of Physics, Gazi University, Teknikokullar, 06500 Ankara, Turkey

^c Nanotechnology Research Center, Department of Physics, Bilkent University, Bilkent, 06800 Ankara, Turkey

^d Department of Electrical and Electronics Engineering, Bilkent University, Bilkent, 06800 Ankara, Turkey

ARTICLE INFO

Available online 14 July 2008

PACS:

73.40.–c

73.50.Dn

73.61.Ey

Keywords:

Parallel conduction

Mixed conduction

Multi-carrier

MODFET

HEMT

QMSA

ABSTRACT

We report a simple method to extract the mobility and sheet carrier densities of conduction channels in conventional modulation doped field-effect transistor (MODFET) structures and unintentionally doped GaN-based high-electron mobility transistor (HEMT) structures for a special case. Extraction of the conduction channels from the magnetic field-dependent data can present number of problems; even the most recent methods encounter great difficulties. For the GaN-based HEMT structures which have lower mobilities and larger effective masses than that of GaAs-based counterparts, these difficulties become more prominent. In this study, we describe a simple method for magnetotransport analysis to extract conduction channels successfully for a special case that is commonly encountered: one bulk channel and one two-dimensional electron gas (2DEG) channel. Advantage of this method is mainly its simplicity. The analysis can be done with only two magnetic field-dependent measurements per temperature step. The method is applied to the magnetotransport results of an unintentionally doped AlGaIn/GaN/AlN heterostructure over a temperature range of 29–350 K and in a magnetic field range of 0–1.5 T ($\mu B < 1$). The results are then compared with those obtained using a commercial package for these calculations namely: quantitative mobility spectrum analysis (QMSA).

© 2008 Elsevier Ltd. All rights reserved.

1. Introduction

GaAs-based modulation doped field-effect transistors (MODFETs), which are based on carrier transfer from a highly doped barrier layer into undoped GaAs or InGaAs layer, are widely used in high-speed device applications [1]. After the excellent performance of GaN-based high-electron mobility transistors (HEMTs) reported by Khan et al., many successful GaN-based HEMTs including MODFETs have been demonstrated [2–4]. These undoped or modulation doped GaN-based HEMTs have received up most attention for their potential use in high-power, high-temperature, microwave and high-frequency applications [5–7]. Because the mobility and the carrier density of the two-dimensional electron gas (2DEG) are the two key parameters in these applications, a precise calculation of these parameters is very important. However, in the presence of multiple carrier species, mixed-conduction effects may have a strong influence on the electronic properties of HEMTs [8]. In the single magnetic field Hall measurements, it is assumed that all carriers in different

conducting channels have the same drift velocity. In GaAs-based MODFETs and GaN-based HEMTs including MODFETs, there can be strong parallel bulk conduction due to modulation doping. This may even be present in unintentional doped material [9,10]. In order to separate the 2DEG and the parallel bulk contributions from each other, an alternative measurement technique and different method for the analysis of results are needed.

The analysis of magnetic field-dependent resistivity and Hall data have been discussed in several papers for the parallel conduction problem [11–13]. The traditional techniques for magnetic field-dependent Hall data are two-carrier model [14] or the multi-carrier fitting procedure (MCF) [15,16] which have shortcomings about the need of prior assumptions of approximate mobilities and carrier densities of the carriers. To overcome such shortcomings, mobility spectrum analysis (MSA) is proposed by Beck and Andersson [17]. In 1993, Meyer et al. [8] proposed a hybrid model which uses both MCF and MSA. In 1992, Dziuba and Gorska [18] proposed another mobility spectrum method which generates optimized quantitative results with the experimental results. This method later used in the commercial quantitative mobility spectrum analysis (QMSA) package [19]. The QMSA method has been used extensively for a number of different material systems including GaAs- and GaN-based heterostructures [10,20–22]. However, in order to extract the

* Corresponding author at: Department of Computing and Electronic Systems, University of Essex, CO4 3SQ Colchester, UK.

E-mail address: sblisesivdin@gmail.com (S.B. Lisesivdin).

effect of low-mobility bulk carriers, very large magnetic fields ($\mu_{\min}B_{\max} \gg 1$) and stable thermal conditions required for long durations during the Hall measurements.

In this work, we propose a simple method for parallel conduction in MODFETs and GaN-based HEMTs. The results are compared with those obtained using the QMSA method.

2. Theoretical considerations

Motion of the carriers in a Hall sample can be explained using the equations:

$$\begin{aligned} J_x &= \sigma_{xx}E_x + \sigma_{xy}E_y \\ J_y &= \sigma_{yx}E_x + \sigma_{yy}E_y \end{aligned} \quad (1)$$

where $\sigma_{xx} = \sigma_{yy}$ and $\sigma_{xy} = \sigma_{-yx}$ are longitudinal and transverse conductivity tensor components, respectively. Experimental mobility and carrier density are related to conductivity tensor components through the following equations [13]:

$$\begin{aligned} \sigma_{xx} &= \frac{nq\mu}{1 + \mu^2 B^2} & \rightarrow \text{for } m \text{ channels } \rightarrow & \sigma_{xx} = \sum_{i=1}^m \frac{n_i q \mu_i}{1 + \mu_i^2 B^2} \\ \sigma_{xy} &= \frac{nq\mu^2 B}{1 + \mu^2 B^2} = \sigma_{xx} \mu B & & \sigma_{xy} = \sum_{i=1}^m \frac{n_i q \mu_i^2 B}{1 + \mu_i^2 B^2} \end{aligned} \quad (2)$$

where n_i and μ_i are the density and mobility of carriers in the i th carrier, respectively. In order to study behaviors of conductivity tensors in HEMT-like structure, some assumptions are made through this study:

- (1) There are two main contributions to conductivity in an HEMT structure: 2DEG, and bulk carriers.
- (2) At the low temperatures, bulk carriers are assumed to be frozen. Therefore, the measured carrier density at the lowest temperature is simply that of the 2DEG.
- (3) Because of the 2DEG carrier density is temperature independent [23]; the temperature dependence of the measured carrier density is associated with the bulk carriers only.
- (4) Densities of bulk carriers and the 2DEG are in the same order.

Firstly, magnetic field-dependent conductivity tensors are investigated for two-carrier situation. Carrier 2 is assumed to be the bulk carrier with $\mu_2 = 0.088 \text{ m}^2/\text{V s}$, $n_2 = 8 \times 10^{20} \text{ m}^{-3}$ which

are quite typical values for the GaN-based HEMT structures [20]. The carrier 1 is the 2DEG carrier with the same carrier density but has greater mobility. For the $\mu_1/\mu_2 = 1.5, 2$ and 3 situations, conductivity tensors of the carriers and the total conductivity tensors are shown in Fig. 1.

It is clear from Fig. 1(a) that the total longitudinal conductivity at high magnetic fields ($B \gg 1$) is dominated by the carrier 2 with the increasing μ_1/μ_2 . We find from Eq. (2)

$$\sigma_{xx}^{\text{Tot}} = \frac{n_2 q \mu_2}{1 + \mu_2^2 B^2} \cong \frac{n_2 q}{\mu_2 B^2} \cong \frac{n_H q \mu_H}{1 + \mu_H^2 B^2} \quad (3)$$

$$\mu_2 \cong \mu_H \frac{n_H - n_1}{n_H} \quad (4)$$

The magnetic field-dependent derivative of conductivity tensors are investigated for the same situations. Derivative of the conductivity tensors can be found as

$$\begin{aligned} \sigma'_{xx} &= \frac{2nq\mu^3 B}{(1 + \mu^2 B^2)^2} \\ \sigma'_{xy} &= \frac{nq\mu^2(1 - \mu^2 B^2)}{(1 + \mu^2 B^2)^2} \end{aligned} \quad (5)$$

In Fig. 2, for the derivative of conductivity tensors of the carriers and the derivative of total conductivity tensors for $\mu_1/\mu_2 = 1.5, 2$ and 3 are plotted versus B . At very low magnetic fields ($B \approx 0$), it is clear from Fig. 1(b) that the derivative of total transverse conductivity tensor is more strongly dominated by the carrier 1 with the increasing μ_1/μ_2 . Therefore, from Eq. (2)

$$\sigma_{xy}^{\text{Tot}} = n_1 q \mu_1^2 \cong n_H q \mu_H^2 \quad (6)$$

$$\mu_1 \cong \mu_H \sqrt{\frac{n_H}{n_1}} \quad (7)$$

Because of Eq. (4) is valid at high magnetic fields and Eq. (7) is valid at low magnetic fields only, the results can be re-arranged as

$$\mu_1 \cong \mu_H^{\text{Lo}} \sqrt{\frac{n_H^{\text{Lo}}}{n_1^{\text{Lo}}}} \quad (8)$$

$$\mu_2 \cong \mu_H^{\text{Hi}} \frac{n_H^{\text{Hi}} - n_1^{\text{Hi}}}{n_H^{\text{Hi}}} = \mu_H^{\text{Hi}} \frac{n_2^{\text{Hi}}}{n_H^{\text{Hi}}} \quad (9)$$

Here $\mu_H^{\text{Lo}}, n_H^{\text{Lo}}, \mu_H^{\text{Hi}}, n_H^{\text{Hi}}$ are μ_H, n_H at low magnetic fields and at high magnetic fields, respectively. For the calculation of

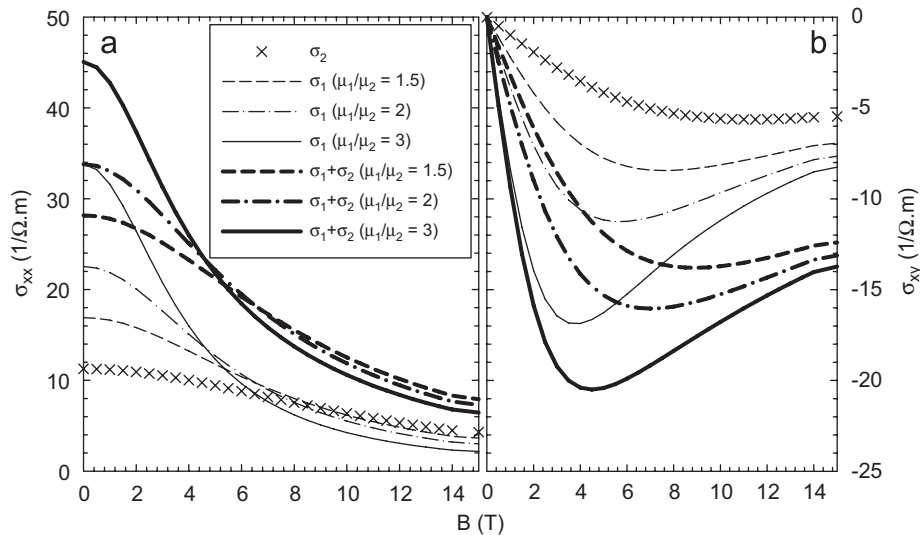


Fig. 1. (a) Longitudinal and (b) transverse conductivities of the carriers and the total conductivity tensors for the situations $\mu_1/\mu_2 = 1.5, 2$ and 3.

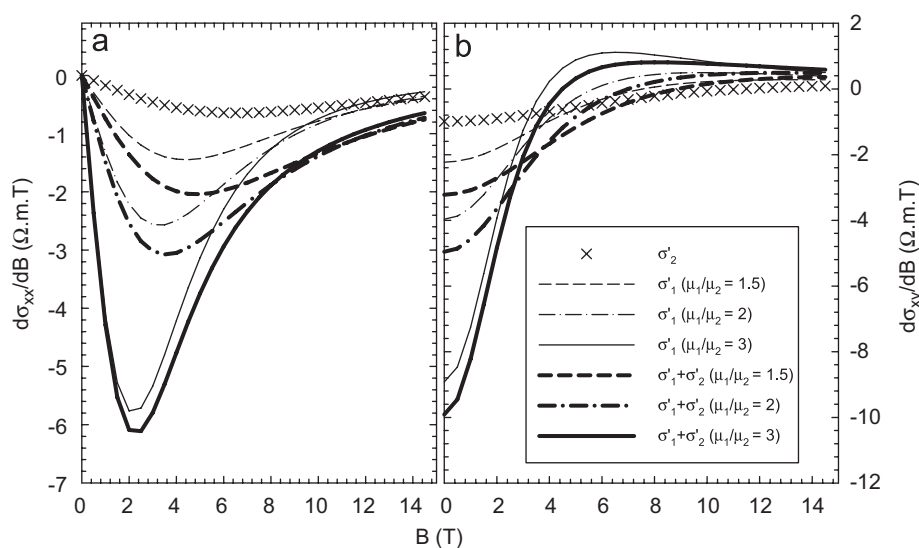


Fig. 2. Derivatives of (a) longitudinal and (b) transverse conductivities of the carriers and the derivatives of total conductivity tensors for the situations $\mu_1/\mu_2 = 1.5, 2$ and 3 .

temperature-independent 2DEG carrier densities of the carrier 1, $n_1^{\text{Lo}} = n_{\text{H}}^{\text{Lo}}$ and $n_1^{\text{Hi}} = n_{\text{H}}^{\text{Hi}}$ can be measured at the lowest temperature available. For all the temperatures of measurement, the conditions, $n_2^{\text{Lo}} = n_{\text{H}}^{\text{Lo}} - n_1^{\text{Lo}}$ and $n_2^{\text{Hi}} = n_{\text{H}}^{\text{Hi}} - n_1^{\text{Hi}}$ can be used.

3. Experimental results

The samples in this study were all grown on *c*-plane (0001) sapphire (Al_2O_3) substrate with a low-pressure MOCVD reactor. Hydrogen was used as the carrier gas; trimethylgallium (TMGa), trimethylaluminum (TMAI), and ammonia were used as Ga, Al and N precursors, respectively. The substrate was cleaned in H_2 ambient at 1100°C , and then a 11.2 nm low-temperature (LT) AlN nucleation layer was grown at 795°C with a 50 mbar reactor pressure. After the deposition of the LT-AlN nucleation layer, the wafers were heated to a high temperature (HT) for annealing. For the samples, approximately a $0.72\text{ }\mu\text{m}$ HT-AlN buffer layer was deposited on the annealed nucleation layers at 1135°C with a 25 mbar reactor pressure. After the deposition of buffer layers, approximately a $2.77\text{ }\mu\text{m}$ HT-GaN layer was grown at the same temperature. Finally, 1-nm-thick AlN interlayer, a 18.8-nm-thick $\text{Al}_{0.25}\text{Ga}_{0.75}\text{N}$ barrier layer, and 10.6 nm GaN cap layer were grown. All layers are nominally undoped.

Ohmic contacts were prepared by the evaporation deposition of Ti/Al/Ni/Au ($200\text{ }\text{\AA}/2000\text{ }\text{\AA}/300\text{ }\text{\AA}/700\text{ }\text{\AA}$) and annealed with rapid thermal annealing (RTA). Ohmic behavior of the contacts was confirmed by the current–voltage (I/V) characteristics. The measurements were taken in a temperature range of $29\text{--}350\text{ K}$ using a Lakeshore Hall effect measurement system (HMS). At temperature steps, the Hall coefficient (with max. 5% error) and resistivity (with max. 0.2% error in the studied range) were measured for both current directions, magnetic field polarizations, and all possible contact configurations for 31 magnetic field steps between 0 and 1.5 T . The magnetic field-dependent data has been analyzed using the QMSA software provided by Lakeshore and the simple parallel conduction extraction method (SPCEM) which is explained in this study.

Resistivity and Hall Effect measurements of $\text{Al}_{0.25}\text{Ga}_{0.75}\text{N}/\text{AlN}/\text{GaN}/\text{AlN}$ heterostructures have been carried out as a function of temperature ($29\text{--}350\text{ K}$) and magnetic field ($0\text{--}1.5\text{ T}$). Fig. 3 shows the temperature-dependent Hall mobility at 0.4 T (filled circles), temperature-dependent mobilities of two carriers calculated

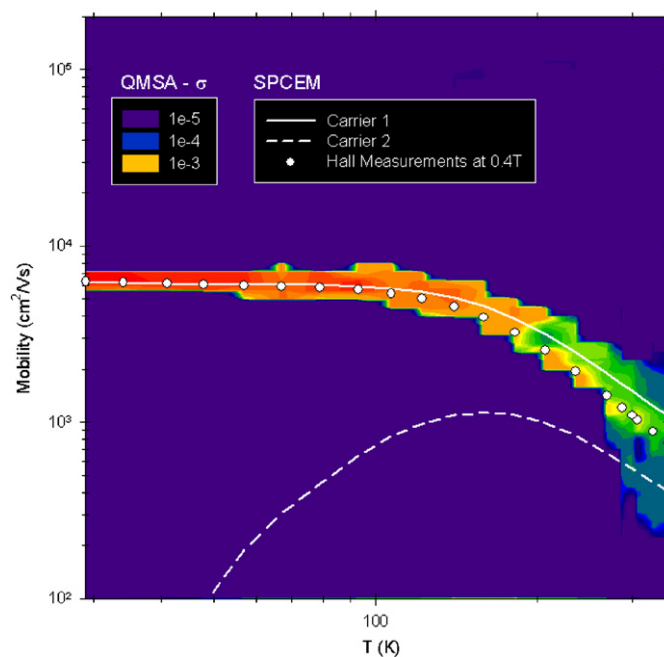


Fig. 3. Temperature-dependent Hall mobility (filled circles), SPCEM results (lines) and QMSA results (3D contour graph).

using the SPCEM (lines) and temperature-dependent mobility spectrum calculated using QMSA (3D contour graph) in the temperature range of $29\text{--}350\text{ K}$. At room temperature, Hall mobility is $1095\text{ cm}^2/\text{Vs}$ and at 20 K , Hall mobility is as high as $6265\text{ cm}^2/\text{Vs}$. Single dominant channel is indicated with the QMSA technique. This channel becomes exactly same with the Hall mobility at low temperatures, while at high temperatures it diverges. At very high temperatures, a small, low-mobility contribution is observed. Same analysis is carried out with SPCEM using the low magnetic field (0.05 T) and high magnetic field (1.5 T) Hall data as the input. It is evident from Fig. 3 that the high-mobility channel results are consistent with the QMSA results. In addition, at temperatures above 50 K , a low-mobility channel is observed which is also consistent with QMSA low-mobility channel at very high temperatures. Based on QMSA and SPCEM results, it is clear that the high-mobility channel is typical of 2DEG

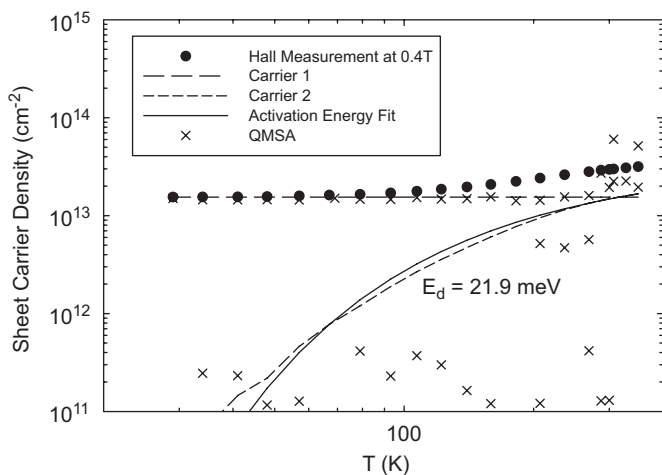


Fig. 4. Temperature-dependent Hall mobility (filled circles), SPCEM results (dashed lines) and QMSA results (crosses). Single donor activation energy fit is shown fit full line.

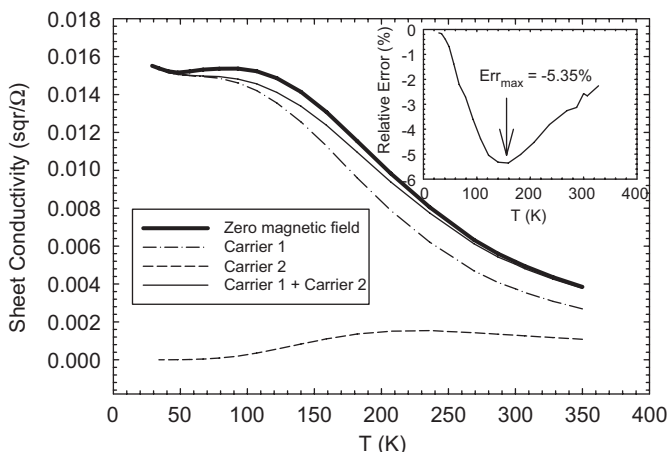


Fig. 5. Zero magnetic field conductivity and conductivities calculated using SPCEM. Inset: relative error of total conductivity which is calculated using SPCEM.

and that the electron mobility is weakly increasing function of decreasing temperature at low temperatures. However, the low-mobility channel is typical of bulk carriers where the electron mobility is decreasing function of decreasing temperature below 200 K due to increased impurity scatterings. At high temperatures the mobilities in both channels decrease rapidly as a result of polar optic scattering.

In Fig. 4, temperature-dependent sheet carrier densities taken from Hall measurements, together with the SPCEM and QMSA results are shown. High-mobility carriers have temperature-independent carrier densities which is typical for 2DEG. QMSA results of the 2DEG is exactly temperature independent, so 2DEG carrier density used in SPCEM is totally consistent with QMSA. In some applications, QMSA may be used to extract bulk carriers successfully [21], however, sometimes it may fail to extract the exact information bulk carriers like this study due to very low mobilities and/or low-magnetoresistivity properties of the material system [24]. Using SPCEM analysis, we find a donor activation energy (E_d) of 21.9 meV for the bulk carriers. Temperature-dependent carrier density investigated with Götz et al.'s [25] two-donor model is close in behavior to our analysis where we used a single-carrier solution. The binding energy that we obtained is very close to hydrogenic donor binding energies

(~ 30 meV) [26]. Because of the samples investigated in our study are unintentionally doped, the observed activation energy may be related oxygen or carbon impurity-related donors, as also reported by Lin et al. [27].

In Fig. 5, zero magnetic field conductivity and conductivities calculated using SPCEM analysis are shown. 2DEG conductivity is dominant especially at low temperatures. Total conductivity calculated with SPCEM has a maximum $\sim 5\%$ error in the investigated temperature range. Because the bulk carriers freeze out at low temperatures (assumption 2) and high bulk carrier densities at high temperatures (assumption 4), SPCEM is successful at both ends of the investigated temperature range.

4. Conclusion

In this work, a SPCEM is formulated and proposed to obtain information about individual parallel conduction channels in GaAs-based MODFETs and GaN-based HEMTs. SPCEM is applied to $\text{Al}_{0.25}\text{Ga}_{0.75}\text{N}/\text{AlN}/\text{GaN}/\text{AlN}$ heterostructures and results are compared with QMSA method. Results are in good agreement with the QMSA. Using the SPCEM analysis, $E_d = 21.9$ meV is found for the donor impurity binding energy for the investigated heterostructures. This value is in agreement with those reported in literature. For single 2DEG and single bulk channel condition, SPCEM gives exact temperature-dependent mobilities and carrier densities of the channels. Unlike QMSA, SPCEM needs only two magnetic field measurements per temperature step. However, the technique is limited to only two conducting channels with a single 2DEG and single bulk carrier channels. For applications to more channels, both the model and the measurements become complicated and involve the use of SdH measurements at different temperatures.

Acknowledgements

This work is supported by the State of Planning Organization of Turkey under Grant no. 2001K120590, and by TUBITAK under Project nos. 104E090, 105E066, 105A005. Ekmel Ozbay acknowledges partial support from the Turkish Academy of Sciences and Sefer Bora Lisesivdin acknowledges 2214 coded international research scholarship from TUBITAK.

References

- [1] J.-H. Tsai, T.-Y. Weng, K.-P. Zhu, Superlatt. Microstruct. 43 (2008) 73.
- [2] M. Asif Khan, J.N. Kuznia, J.M. Van Hove, N. Pan, J. Carter, Appl. Phys. Lett. 60 (1992) 3027.
- [3] Y.-F. Wu, S. Keller, P. Kozodoy, B.P. Keller, P. Parikh, D. Kapolnek, S.P. Denbaars, U.K. Mishra, IEEE Electron. Device Lett. 18 (1997) 290.
- [4] O. Aktas, Z.F. Fan, A. Botchkarev, S.N. Mohammad, M. Roth, T. Jenkins, L. Kehias, H. Morkoc, IEEE Electron. Device Lett. 18 (1997) 293.
- [5] Z. Fan, C. Lu, A.E. Botchkarev, H. Tang, A. Salvador, O. Aktas, W. Kim, H. Morkoc, Electron. Lett. 33 (1997) 814.
- [6] U.K. Mishra, Y.-F. Wu, B.P. Keller, S. Keller, S.P. DenBaars, IEEE Trans. Microwave Theory Tech. 46 (1998) 756.
- [7] N. Maeda, T. Saitoh, K. Tsubaki, T. Nishida, N. Kobayashi, Jpn. J. Appl. Phys. 38 (1999) L799.
- [8] J.R. Meyer, C.A. Hoffman, F.J. Bartoli, D.J. Arnold, S. Sivananthan, J.P. Faurie, Semicond. Sci. Technol. 8 (1993) 805.
- [9] E.F. Schubert, K. Ploog, H. Dämbkes, K. Heime, Appl. Phys. A 33 (1984) 63.
- [10] I. Vurgaftman, J.R. Meyer, C.A. Hoffman, D. Redfern, J. Antoszewski, L. Farone, J.R. Lindemuth, J. Appl. Phys. 84 (1998) 4966.
- [11] J.S. Kim, D.G. Seiler, W.F. Tseng, J. Appl. Phys. 73 (1993) 8324.
- [12] A. Wolkenberg, T. Przeslawski, J. Kaniewski, K. Reginski, J. Phys. Chem. Solids 64 (2003) 7.
- [13] J. Antoszewski, L. Faraone, I. Vurgaftman, J.R. Meyer, C.A. Hoffman, J. Electron. Mater. 33 (2004) 673.
- [14] M.J. Kane, N. Apsley, D.A. Anderson, L.L. Taylor, T. Kerr, J. Phys. C: Solid State Phys. 18 (1985) 5629.

- [15] M.C. Gold, D.A. Nelson, *J. Vac. Sci. Technol. A* 4 (1986) 2040.
- [16] S.P. Tobin, G.N. Pultz, E.E. Krueger, M. Kestigian, K.K. Wong, P.W. Norton, *J. Electron. Mater.* 22 (1993) 907.
- [17] W.A. Beck, J.R. Anderson, *J. Appl. Phys.* 62 (1987) 541.
- [18] Z. Dziuba, M. Gorska, *J. Phys. III Fr.* 2 (1992) 110.
- [19] J. Antoszewski, D.J. Seymour, L. Faraone, J.R. Meyer, C.A. Hoffman, *J. Electron. Mater.* 24 (1995) 1255.
- [20] N. Biyikli, J. Xie, Y.-T. Moon, F. Yun, C.-G. Stefanita, S. Bandyopadhyay, H. Morkoç, I. Vurgaftman, J.R. Meyer, *Appl. Phys. Lett.* 88 (2006) 142106.
- [21] S.B. Lisesivdin, A. Yildiz, S. Acar, M. Kasap, S. Ozcelik, E. Ozbay, *Appl. Phys. Lett.* 91 (2007) 102113.
- [22] S.B. Lisesivdin, A. Yildiz, S. Acar, M. Kasap, S. Ozcelik, E. Ozbay, *Physica B* 399 (2007) 132.
- [23] J.H. Davies, *The Physics of Low-Dimensional Semiconductors*, Cambridge University Press, Cambridge, UK, 1998, p. 332.
- [24] C.H. Swartz, R.P. Tompkins, N.C. Giles, T.H. Myers, H. Lu, W.J. Schaff, L.F. Eastman, *J. Cryst. Growth* 269 (2004) 29.
- [25] W. Götz, N.M. Johnson, C. Chen, H. Liu, C. Kuo, W. Imler, *Appl. Phys. Lett.* 68 (1996) 3144.
- [26] D.C. Look, Z.-Q. Fang, B. Clafin, *J. Cryst. Growth* 281 (2005) 143.
- [27] J.C. Lin, Y.K. Su, S.-J. Chang, W.R. Chen, R.Y. Chen, Y.C. Cheng, W.J. Lin, *J. Cryst. Growth* 285 (2005) 481.